Computational Study of Longitudinal Ventilation Control during an Enclosure Fire within a Tunnel

KAI KANG*

Hatch Mott MacDonald
475 Park Avenue South, 10th Floor
New York, NY 10016, USA

ABSTRACT: The purpose of this study is to examine critical ventilation velocity in a tunnel in the presence of an enclosure fire obstruction. The numerical model is first verified using experimental results from an enclosure fire in the absence of a tunnel and from a tunnel fire in the absence of an enclosure. For an enclosure fire within a tunnel, the impact of the enclosure obstruction is studied using numerical simulation and a critical velocity correlation. The results suggest that the correlation based on the hydraulic diameter of the annular area is better than that based on tunnel height. While further experimental validation is needed, such a correlation would be useful in practice.

KEY WORDS: critical velocity, tunnel fire, enclosure fire, CFD.

INTRODUCTION

FOR A TUNNEL fire, smoke generated from the fire could severely impede visibility and evacuation. One of the schemes to control smoke is longitudinal ventilation, which introduces unidirectional airflow along the tunnel axis. Sufficient ventilation capacity is needed to prevent smoke movement upstream of the fire, that is, to prevent *backlayering* (Figure 1). This not only provides a safe escape, but also allows for fire fighting access. When there is no backlayering, the momentum force from longitudinal ventilation balances the momentum induced by the fire. At this point, the ventilation rate (average flow velocity) is often referred to as the *critical velocity*. Critical velocity is, therefore, the minimum ventilation velocity that is able to prevent smoke backlayering in a tunnel fire [1,2].

*E-mail: kai.kang@hatchmott.com

1042-3915/06/03 0159–23 $10.00/0 DOI: 10.1177/1042391506056737

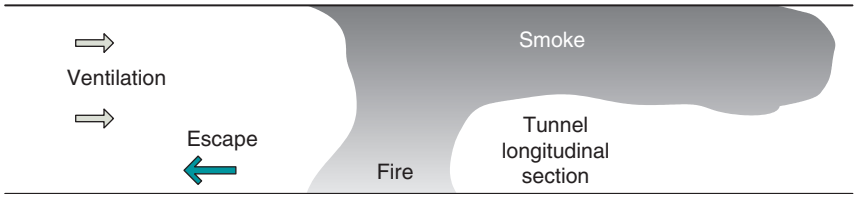

Figure 1. *Tunnel fire and longitudinal ventilation control. (The color version of this figure is available on-line.)*

Many tests have been conducted on longitudinal ventilation control of tunnel fires (refer to the reviews by Grant et al. [3] and Carvel et al. [4]), for example, the memorial tunnel fire and ventilation test program (MTFVTP) [5]. Computational studies have also been conducted to quantify critical velocity in tunnel fires (Rhodes [6], Kennedy and Kang [7], and Tetzner et al. [8], etc.). A pool fire is used widely in tests such as MTFVTP, while in other experiments, such as the small-scale tunnel fire tests by Wu and Bakar [11], a gas fire is used. In a recent study, Kunsch [9,10] reported an analytical formulation of critical velocity, assuming the fire to be point source in a two-dimensional tunnel.

The correlation of critical velocity in [1,2] is based on critical Froude number and a one-dimensional (1D) assumption. Deviations from the 1D assumption usually arise in practice, such as a wider aspect ratio of the tunnel cross section. Recent studies have examined the validity of the critical velocity correlation for wider tunnels [8,11,12]. However, for an in-car fire associated with a stalled train in a tunnel, the effect of the train obstruction on critical velocity is important, but has had few studies in the past. The correlation in [1] used the *net* tunnel annular area to account for the train obstruction, but with no reference or known supporting work. Therefore, the impact of the train obstruction on critical ventilation velocity warrants further investigation.

The in-car fire of a rail vehicle can be related to an enclosure fire with limited openings, for example, Steckler's room fire [13]. The enclosure in Steckler's room fire experiment has a single door opening. At the door centerline, velocity and temperature are measured, for which many numerical comparisons have been made [14–16]. For an enclosure fire within a tunnel, the momentum and heat transfer through the door is important, as it directly interacts with longitudinal ventilation. The term, tunnel enclosure fire, here refers to such an enclosure fire within the tunnel.

The purpose of this study is to examine critical ventilation velocity for an enclosure fire within the tunnel, in particular, the effect of the enclosure obstruction. The numerical results for an enclosure fire are first verified

using data from Steckler's room fire test. One of the small-scale tunnel fire tests by Wu and Bakar [11] is then used to validate the numerical results for a tunnel fire. Finally, the critical velocity correlation [1] is evaluated to incorporate the effect of enclosure obstruction. Note that because of limited experimental data, the approach of *dividing* the problem of a tunnel enclosure fire into an enclosure fire and a tunnel fire is used to confirm the accuracy of the numerical results.

CFD MODELING APPROACH

Mathematical Models

A general purpose CFD software [17], based on the finite volume method is used. The flow field is solved using the Reynolds time-averaging approach, with a standard k–ε turbulence model. Both the equations of kinetic energy, k, and dissipation, ε, include a buoyancy term, G_b. The k–ε equations are given as,

$$\frac{\partial(\rho k)}{\partial t}+\frac{\partial(\rho k u_i)}{\partial x_i}=\frac{\partial}{\partial x_j}\left[\left(\mu+\frac{\mu_t}{\sigma_k}\right)\frac{\partial k}{\partial x_j}\right]+G_k+G_b-\rho\varepsilon-Y_M+S_k, \tag{1}$$

$$\frac{\partial(\rho \varepsilon)}{\partial t}+\frac{\partial(\rho \varepsilon u_i)}{\partial x_i}=\frac{\partial}{\partial x_j}\left[\left(\mu+\frac{\mu_t}{\sigma_\varepsilon}\right)\frac{\partial \varepsilon}{\partial x_j}\right]+C_{1\varepsilon}\frac{\varepsilon}{k}(G_k+C_{3\varepsilon}G_b)-C_{2\varepsilon}\rho\frac{\varepsilon^2}{k}+S_\varepsilon \tag{2}$$

where $C_{1\varepsilon}=1.44$, $C_{2\varepsilon}=1.92$, $C_\mu=0.09$, μ_t is turbulent viscosity, $\mu_t=\rho C_\mu k^2/\varepsilon$, and the turbulent Prandtl numbers $\sigma_k=1.0$, $\sigma_\varepsilon=1.3$. The parameter $C_{3\varepsilon}$ is a computed parameter based on the local flow direction [17]. For an ideal gas, G_b is a function of density variation:

$$G_b=-g_i\frac{\mu_t}{\rho Pr_t}\frac{\partial \rho}{\partial x_i} \tag{3}$$

Fire Models

The Method of VHMS

The method of volumetric heat and mass source (VHMS) is a multiple component transport model. It only considers heat and mass transfer caused by fire. VHMS uses a volumetric energy source for the heat release rate, and a mass source for the fuel. In addition, oxygen consumed can be

explicitly accounted for as a mass sink. An arbitrary reaction can be modeled by VHMS. This method is used in several case studies (e.g., [7,18]).

The Mixture Fraction/PDF Model

This model solves for a conserved scalar, the so called mixture fraction, and avoids solving the transport equation for each component as VHMS does. An assumed shape probability density function (PDF) is calculated in advance, and used as a look-up table by the solver. Given a mixture fraction, the mixture composition and material properties can be derived from PDF. The time-averaged mean and variance of mixture fraction are modeled as:

$$\frac{\partial}{\partial t}\left(\rho\bar{f}\right) + \nabla\cdot\left(\rho\boldsymbol{v}\bar{f}\right) = \nabla\cdot\left(\frac{\mu_t}{\sigma_t}\nabla\bar{f}\right) + S_m + S_{user} \tag{4}$$

$$\frac{\partial}{\partial t}\left(\rho\overline{f'^2}\right) + \nabla\cdot\left(\rho\boldsymbol{v}\overline{f'^2}\right) = \nabla\cdot\left(\frac{\mu_t}{\sigma_t}\nabla\overline{f'^2}\right) + C_g\mu_t\left(\nabla^2\bar{f}\right) - C_d\rho\frac{\varepsilon}{k}\overline{f'^2} + S_{user} \tag{5}$$

where $\sigma_t = 0.85$, $C_g = 2.86$, and $C_d = 2.0$. The value of the term S_m is due to any addition of mass from liquid or solid fuel, and S_{user} is a user-specified source term. The reaction chemistry sub-model used is the stoichiometric flame sheet model, assuming that *mixed is burnt*. A similar approach is implemented in the fire dynamics simulator (FDS) program [20].

Discrete Transfer Radiation Model

The discrete transfer radiation model (DTRM) integrates along a pre-set series of rays emanating from boundary faces, and assumes that surface radiation is isotropic [21]. The scattering coefficient is omitted. The absorption coefficient, a, can be a constant, or a variable using the weighted-sum-of-gray-gases model [17]. Clustering by surface or volume averaging is used to reduce the number of rays and computational cost. The change of radiant intensity, I, as a function of path, s, is,

$$\frac{dI}{ds} + aI = \frac{a\sigma T^4}{\pi} \tag{6}$$

ENCLOSURE FIRE

Description of Enclosure Fire

The enclosure fire considered here is based on Steckler's room fire [13]. The enclosure dimension is $W \times L = 2.8\,\text{m} \times 2.8\,\text{m}$, and $H = 2.18\,\text{m}$ (Figure 2).

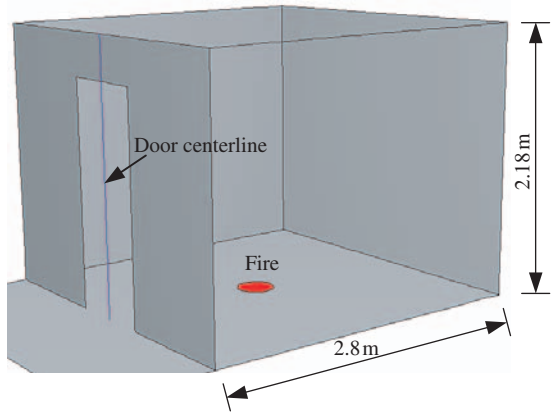

Figure 2. *Schematic of the enclosure fire model. (The color version of this figure is available on-line.)*

A door, 0.74 m wide and 1.83 m high, is in the middle of a sidewall. A circular burner is located in the center, with its top flush with the floor. The diameter of the burner is 0.3 m. Using a bidirectional velocity probe and thermocouple, the horizontal velocity and temperature are measured for each test at the door centerline, with results tabulated in [13].

Fire Scenarios and Numerical Approach

Three fire sizes, 62.9, 105.3, and 158 kW, corresponding to experiments 14, 20, and 21 are evaluated. The fire heat release rate (HRR) is obtained by burning commercial grade methane at a fixed rate. In the experiments, the walls and ceiling are covered with ceramic fiber insulation board to minimize heat loss. Typical thermal properties of ceramic are specific heat, $C_p = 2310\,\mathrm{J/(kg\,K)}$, and conductivity, $k = 0.06\,\mathrm{W/(mK)}$ [22].

The CFD model consists of the enclosure and a small extension of connected space outside the door (Figure 2). Approximately 120–250 k hexahedral control volumes are used. Ambient air temperature is 29°C [13]. Methane's lower heating value is about 50 MJ/kg. The one-step methane–air reaction has an air-fuel mass ratio, $R_{AF} = 17.2$, and is:

$$CH_4 + 2(O_2 + 3.76N_2) \rightarrow CO_2 + 2H_2O + 7.52N_2$$

In the VHMS method, the volumetric fire source is modeled as a cylinder. The cylinder's diameter, which is based on the burner, is 0.3 m, and its height is 0.2 m. For the mixture fraction approach, the methane consumption rate

is determined from HRR and the fuel heat of combustion. The DTRM radiation model is used with the mixture fraction model.

Comparison with Experimental Results

In general, the numerical results are in good agreement with the experimental results for velocity and temperature profiles at the door centerline (Figure 3). The positive sign for horizontal velocity means flow out of the enclosure. For the three HRRs examined, VHMS seems to have

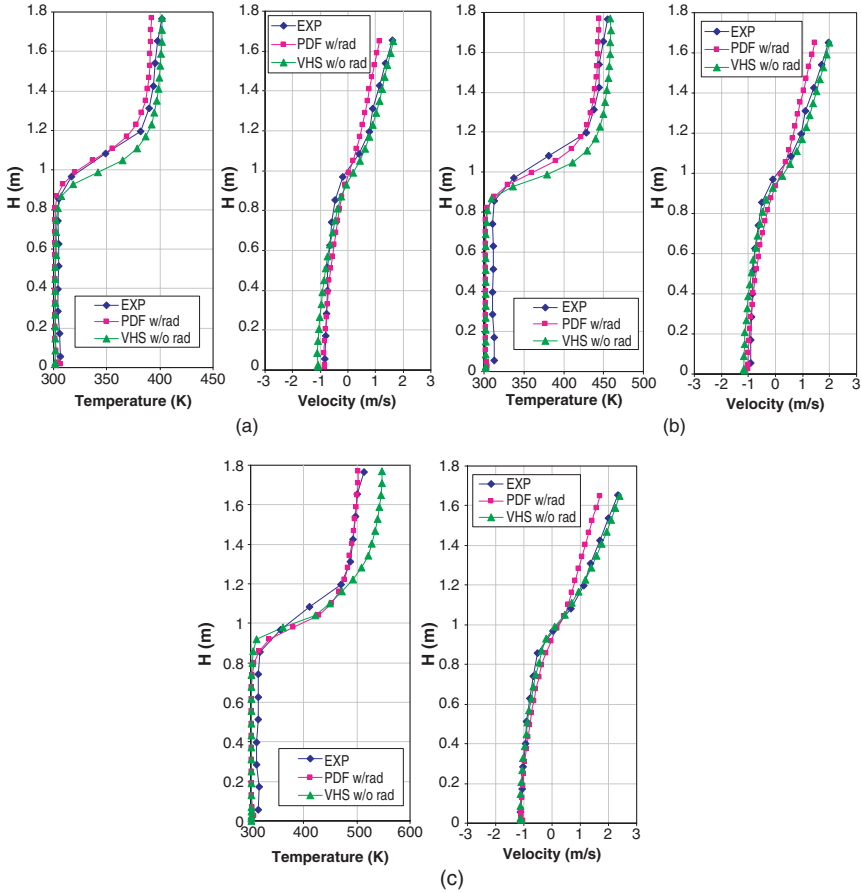

Figure 3. *Comparison of horizontal flow velocity and temperature at door centerline for fire: (a) 62.9 kW; (b) 105.3 kW; and (c) 158 kW. (The color version of this figure is available on-line.)*

Table 1. Comparison between numerical and experiment results.

Fire HRR (kW)	Neutral plane location (h_0/h)	Inflow (kg/s)	Outflow (kg/s)	Average temperature (°C)
62.9				
EXP 14 (Steckler et al. [13])	0.562	0.554	0.571	114
VHMS	0.516	0.619	0.620	117
PDF	0.532	0.468	0.469	103
Lewis et al. [15]	0.546	0.521	0.523	–
PDF (Xue et al. [14])	0.450	1.165	1.209	–
105.3				
EXP 20 (Steckler et al. [13])	0.547	0.618	0.630	161
VHMS	0.516	0.670	0.672	170
PDF	0.514	0.557	0.559	154
158.0				
EXP 21 (Steckler et al. [13])	0.535	0.679	0.606	193
VHMS	0.531	0.666	0.669	228
PDF	0.508	0.602	0.605	202

overpredicted the centerline temperature, but gives good agreement for the velocity, probably because the mass production and consumption rates are explicitly set for the fire source. On the other hand, the mixture fraction approach gives a better prediction of temperature, but underestimates horizontal velocity.

The normalized neutral plane height, h_0/h, the mass inflow and outflow rates, and the centerline averaged temperature above h_0, are shown in Table 1. The horizontal velocity equals zero at neutral plane height, h_0 [13]. For Steckler's room fire of 62.9 kW, Xue et al. [14] evaluated the volumetric heat source (VHS), the eddy break-up model, and the mixture fraction/PDF model. Lewis et al. [15] obtained good agreement with the experimental results; however, the PDF model by Xue et al. [14] did not show the same consistency. Note that the current numerical results are reasonably close to the experimental results. The largest discrepancy is in the mass flow rate for $Q = 62.9$ kW, predicted by PDF, which is about 15% lower. Overall, the numerical results are within about $\pm 10\%$ of the experimental measurements.

Figure 4 is the temperature distribution in the symmetry plane with HRR 62.9 kW. It shows that the fire tilts towards the back wall, forced by the makeup air through the door. The difference in Figure 4 is because of the two fire models. In VHMS, the height of the cylindrical volumetric source is defined arbitrarily, while in contrast, the mixture fraction approach relies on turbulent mixing, and takes into account oxygen availability. The near-field prediction needs further validation. However, for an enclosure fire within

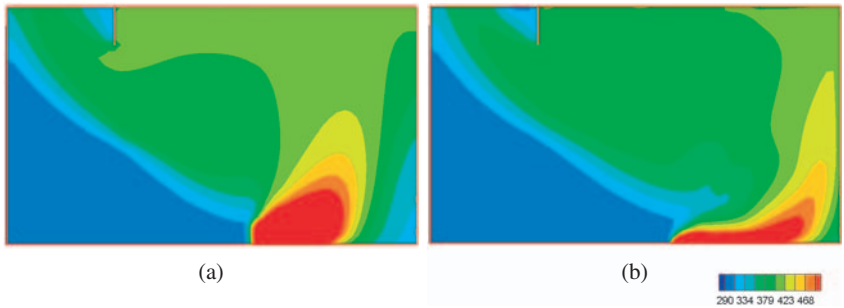

Figure 4. *Temperature distribution in the enclosure center plane, predicted by: (a) VHMS and (b) mixture fraction/PDF model, Q = 62.9 kW. (The color version of this figure is available on-line.)*

the tunnel, the airflow and heat transfer through the enclosure door are more relevant to longitudinal ventilation. Therefore, the agreement with the experimental results provides a verification of the numerical approach to further evaluate tunnel enclosure fire.

ENCLOSURE FIRE WITHIN A TUNNEL

The enclosure fire considered above can be related to a rail vehicle fire in a tunnel. For fires in a tunnel, longitudinal ventilation is often used to arrest the hot gas and smoke to prevent backlayering (Figure 1). As discussed above, the effect of an enclosure obstruction on critical ventilation velocity is of practical importance, but is not well understood. In this section, a brief review of the correlation of critical velocity (CV) is given first, followed by the verification of the numerical results on a tunnel fire using experimental results [11]. The effect of enclosure obstruction is then examined using the same small-scale tunnel model.

Correlations of Critical Velocity

Two formulae are focused on here. The first one is from the subway environmental simulation program [1],

$$V_c = K_g \left(\frac{gHQ}{Fr_c \rho_0 C_p A T_f} \right)^{1/3} \tag{7}$$

$$T_f = \frac{Q}{\rho_0 C_p A V_c} + T_0 \tag{8}$$

where the critical Froude number, $Fr_c = 4.50$, and the tunnel grade (ω) correction factor K_g is,

$$K_g = 1 + 0.0374 \cdot (\omega)^{0.8} \tag{9}$$

The other formula is a dimensionless correlation from the small-scale experiments [11], and is based on that by Oka and Atkinson [23],

$$V_c^* = 0.40 \cdot \left(\frac{Q^*}{0.20}\right)^{1/3} \quad \text{for } Q^* \leq 0.20, \tag{10}$$

and

$$V_c^* = 0.40 \quad \text{for } Q^* > 0.20 \tag{11}$$

where the dimensionless HRR, Q^*, and the dimensionless critical velocity, V_c^*, are given by,

$$V_c^* = \frac{V}{\sqrt{gH_D}} \tag{12}$$

$$Q^* = \frac{Q}{\rho_0 C_p T_0 g^{1/2} H_D^{5/2}} \tag{13}$$

The correlation of CV by Oka and Atkinson [23] is slightly different from that given in [1]. It uses tunnel height instead of hydraulic diameter, and the limit of Q^* is 0.12. For the nine burners tested in [23], the right-hand coefficient in Equations (10) and (11) varies from 0.22 to 0.38, whereas the constant of 0.40 is based on a single burner [11]. Further details of CV correlations and Froude modeling can be found in Grant et al. [3].

Description of Tunnel Enclosure Fire Model

Figure 5 depicts the small-scale tunnel model by Wu and Bakar [11]. The tunnel is 15 m long, with a square cross section of 250 mm. The wall upstream and downstream of the fire is made from 6.25 mm thick transparent acrylic sheet (PMMA), and 1.25 mm thick stainless steel, respectively. Propane gas is supplied through a circular burner, about 6 m from the entrance portal (Figure 5(a)). The diameter of the burner is 106 mm.

Figure 5 also shows the enclosure obstruction. Three blockage ratios are considered, $\phi = 25$, 50, and 65%. Blockage ratio is the ratio of enclosure frontal area to tunnel cross-sectional area. A 25% blockage ratio can be

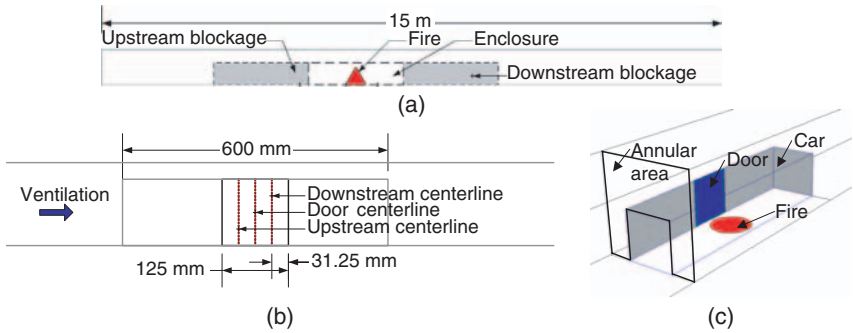

Figure 5. *(a) Tunnel fire model after Wu and Bakar [11], dashed lines indicate enclosure and solid blockage; (b) schematic of enclosure, with locations of door centerline, upstream centerline, and downstream centerline; and (c) enclosure fire within a tunnel. (The color version of this figure is available on-line.)*

related to a road tunnel, whereas 50% and 65% can be related to a rail tunnel. The enclosure length is 600 mm, and the aspect ratio of width to height is one. There is a full-height opening, 125 mm wide, in the middle of one sidewall, facing the fire inside the enclosure (Figure 5(c)). Figure 5(b) shows the centerlines on the enclosure door. The upstream centerline is the centerline of the left half of the door, similarly for the downstream centerline. Solid blockage, either upstream or downstream of the enclosure (Figure 5(a)), is considered in addition to enclosure obstruction. The solid blockage has the same length as the enclosure. Highlighted in Figure 5(c) is the *net* transverse section at 25% blockage ratio, which is referred to as annular area.

The enclosure is modeled as a zero-thickness steel shell. The enclosure allows heat transfer across the tunnel, and its door is the only flow path to the tunnel. Fire is simulated using the mixture fraction approach with DTRM. For a tunnel fire without an enclosure obstruction, three fire sizes, 7.5, 15, and 25 kW, are evaluated and for an enclosure fire obstruction within a tunnel, 7.5 and 15 kW are considered. Using the scaling procedure, 7.5 and 15 kW are equivalent to about 13 and 27 MW in a tunnel of 5 m by 5 m. The propane gas reaction, shown below, has an enthalpy change of 46.4 MJ/kg,

$$C_3H_8 + 5O_2 \rightarrow 3CO_2 + 4H_2O$$

Critical Ventilation Velocity for Fire in a Tunnel

A tunnel fire without an enclosure obstruction is examined first to verify the numerical model. The critical ventilation velocity, as a function of HRR,

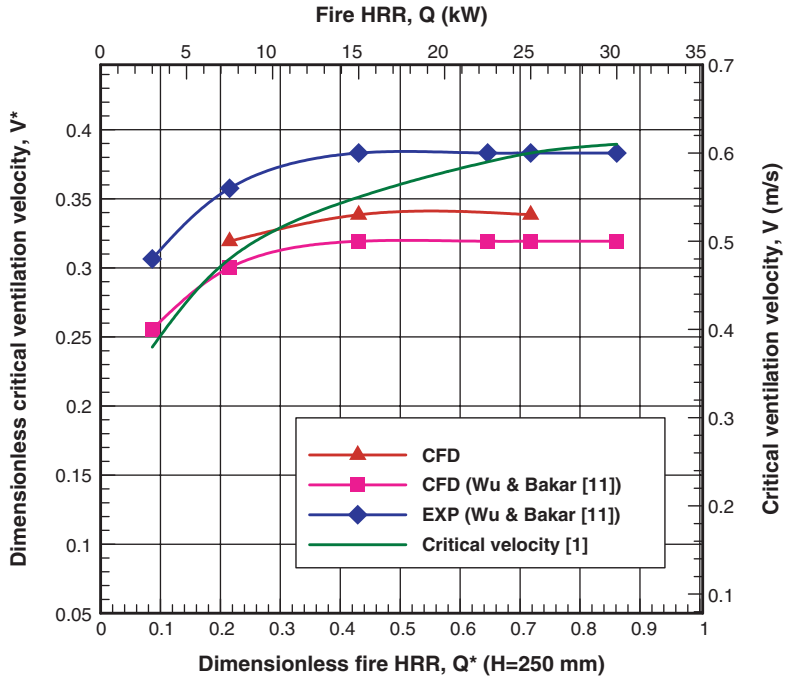

Figure 6. *Comparison of critical ventilation velocity for different HRR. (The color version of this figure is available on-line.)*

is compared with the results by Wu and Bakar [11] and the CV formula, Equation (7), in Figure 6. The primary axes are dimensionless based on tunnel height, $H = 250$ mm, and the secondary are in dimensional form. The results indicate that critical velocity, V_c, is proportional to $Q^{1/3}$ up to a certain limit, and then becomes independent of Q. This asymptotic behavior has been confirmed by many other tests, such as Megret et al. [24]. The current results are in reasonably good agreement with those in [11], particularly with the numerical results.

Note that Equations (10) and (11) are based on the experimental results in Figure 6. The difference between the two CV expressions, Equations (7) and (10), can be explained as follows. Substituting Equations (12) and (13) into Equation (10) to eliminate the dimensionless parameters, gives,

$$V_c = 0.684 \cdot \left(\frac{gQ}{\rho_0 C_p T_0 H_D} \right)^{1/3} \tag{14}$$

and for the given tunnel, with $W = A/H$ and $W = H = H_D$, Equation (7) is then

$$V_c = 0.606 \cdot \left(\frac{gQ}{\rho_0 C_p T_f W} \right)^{1/3} \tag{15}$$

Equation (14) has a larger coefficient, and uses ambient air temperature, instead of hot gas bulk temperature, T_f, in Equation (15). In addition, Equation (14) has an 'arbitrary' limit (Equation (11)). As a result, Equation (14), or the experimental results show higher critical ventilation velocity up to $Q^* = 0.7$ or $Q = 25\,\text{kW}$ (Figure 6).

Among others, Kennedy and Kang [7] also noticed the difference between the numerical results and the correlation (Equation (15)). For the range of HRR considered, CFD predicts a 'super' critical velocity independent of HRR, but the CV correlation does not. Wu and Bakar [11] attributed super critical velocity to the combined effects of air entrainment, thermal resistance of fire, and McCaffrey's fire plume theory. As HRR increases, fire poses higher thermal resistance to ventilation, but it also means higher air entrainment. The existence of super critical velocity indicates certain constraints on the fire-induced momentum. As shown in Figure 6, the fire-induced momentum might be constrained between 0.22 and 0.43 for Q^*, or 7.5 kW and 15 kW. For the generality of the limit of Q^*, a statistical approach, similar to that used for tunnel fire HRR [4] might be useful.

Critical Ventilation Velocity for Enclosure Fire in a Tunnel

For an enclosure fire within a tunnel, the fire-induced flow is important. With no fire, velocity profiles at the door centerline, upstream centerline, and downstream centerline are shown in Figure 7, for a blockage ratio of 25%, and ventilation velocity of 0.35 m/s. A typical transverse flow speed, the secondary flow across the door, is less than 10% of the longitudinal flow speed, 0.20 m/s (Figure 7). In contrast, with a 15 kW enclosure fire, the transverse flow is dominated by the fire (Figure 8). The flow speeds in the transverse and the longitudinal direction are comparable, for example, 1.30 versus 1.35 m/s at the downstream centerline. In the longitudinal direction, the maximum speed occurs in the lower half of the door, whereas it is near the top of the enclosure when there is no fire.

The interaction of fire-induced flow and longitudinal ventilation generates a swirl flow motion at the door, inside the enclosure, and in the downstream tunnel section. This is visualized in Figure 9 by pathlines starting from the selected locations at the door. Qualitatively, it shows the eddy structure inside the enclosure, the lift-off and the lateral spiral flow

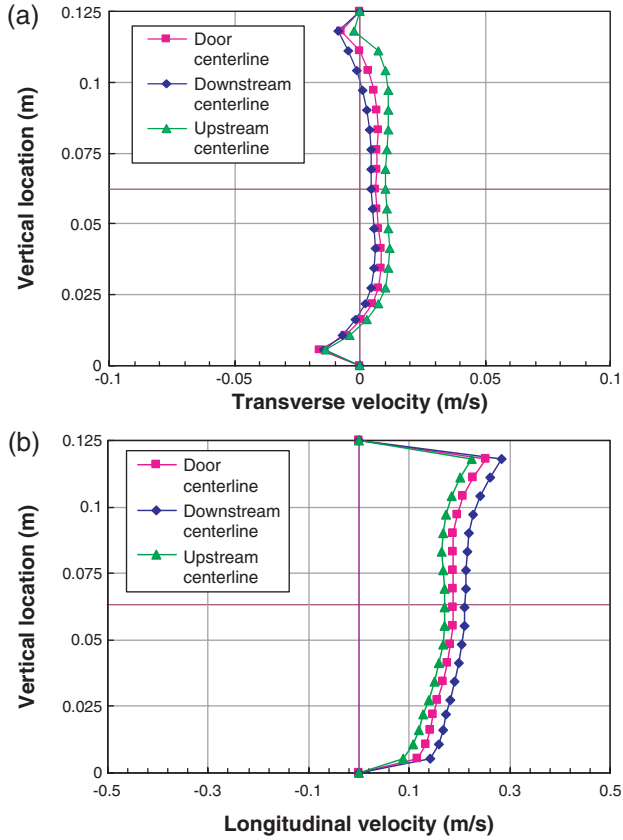

Figure 7. *Predicted (a) transverse velocity and (b) longitudinal velocity at door centerline, upstream centerline, and downstream centerline, no fire, $\phi = 25\%$, and $V = 0.35$ m/s. (The color version of this figure is available on-line.)*

pattern. Such an interaction could be important in the control of backlayering. Previously, Equation (7) was revised using the annular area instead of the entire cross-sectional area [1,7], that is, $A_a = A - A_b$. The calculated CV is thus based on annular area (Figure 5(c)).

It should be noted that the CV correlation (Equation (7)) was derived from the modified Froude number [2], Fr_m, defined as [25],

$$Fr_m = \left(\frac{gH\Delta T}{U^2 T} \right) \tag{16}$$

and Froude number, $Fr = U^2/(gH)$, is the ratio of inertia force over gravity force, in which H is the characteristic length scale. Thomas's study on the

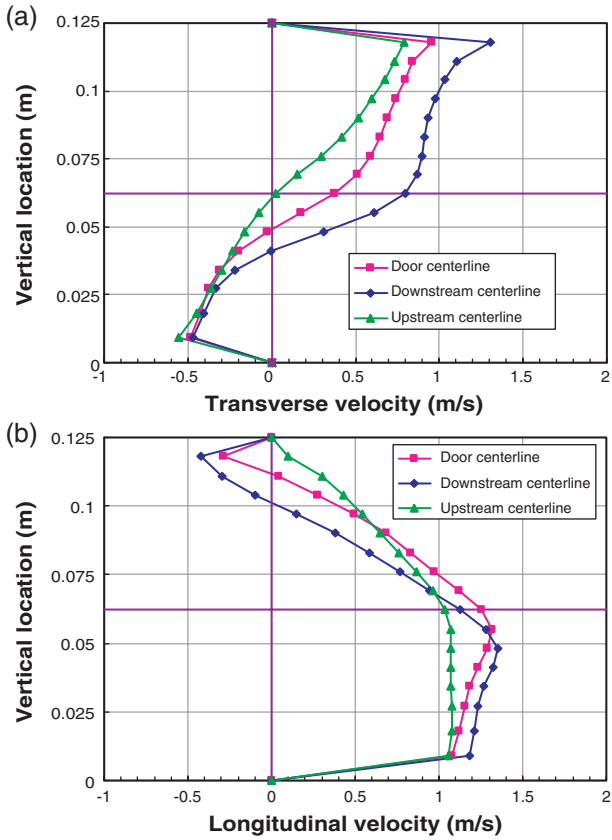

Figure 8. *Predicted (a) transverse velocity and (b) longitudinal velocity at door centerline, upstream centerline, and downstream centerline, $Q = 15$ kW, $\phi = 25\%$, and $V = 0.35$ m/s. (The color version of this figure is available on-line.)*

fire plume used the height as the characteristic length scale, and the same is used in Equation (7). This is reasonable for a tunnel fire without obstruction. However, for an enclosure fire within a tunnel, the hydraulic diameter of the tunnel annular area better characterizes the hydrodynamic interaction of the fire-induced flow and longitudinal ventilation. Therefore, it is proposed that the hydraulic diameter be used for CV correlation, that is,

$$V_c = K_g \left(\frac{g H_D Q}{Fr_c \rho_0 C_p A_a T_f} \right)^{1/3} \tag{17}$$

$$T_f = \frac{Q}{\rho_0 C_p A_a V_c} + T_0, \tag{18}$$

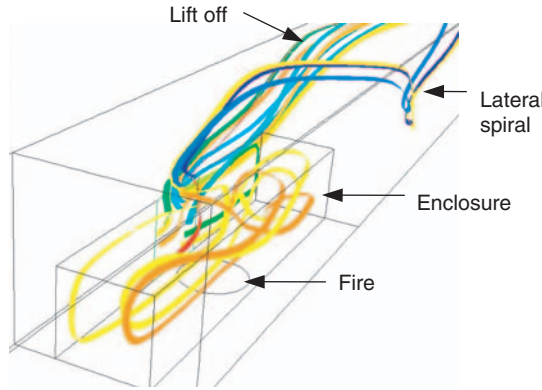

Figure 9. *Visualization of flow pathlines from the enclosure door, $Q = 15\,kW$, $\phi = 25\%$, and $V = 0.35\,m/s$. (The color version of this figure is available on-line.)*

and

$$H_D = \frac{2 \times (A - A_b)}{2 \times \sqrt{A} + \sqrt{A_b}} \tag{19}$$

where the annular area, $A_a = A - A_b$, and the hydraulic diameter, H_D, is the ratio of four times the annular area to the wetted perimeter.

Figure 10 compares the calculated CV based on hydraulic diameter (Equation (17)) and tunnel height (Equation (7)), as a function of enclosure blockage ratio. A clear deviation can be seen, as the correlation based on tunnel height shows that CV increases as blockage ratio increases, while that based on hydraulic diameter shows the opposite. Significant higher critical velocity is predicted using tunnel height than that using hydraulic diameter, for example, about 50% higher at a blockage ratio of 50%. For blockage ratios of 25, 50, and 65%, Figure 10 also shows that the numerical results agree with those based on hydraulic diameter.

In addition, the effect of both fire HRR and blockage ratio is compared with the two CV correlations (Figure 11). As blockage ratio increases, the calculated CV based on hydraulic diameter converges, and becomes less dependent on HRR. Indeed, assume $T_f \gg T_0$, ignore T_0 in Equation (18), and substitute the expression for $A_a \cdot T_f$ from Equation (18) into Equation (17), which gives,

$$V_c \propto (H_D)^{1/2}, \tag{20}$$

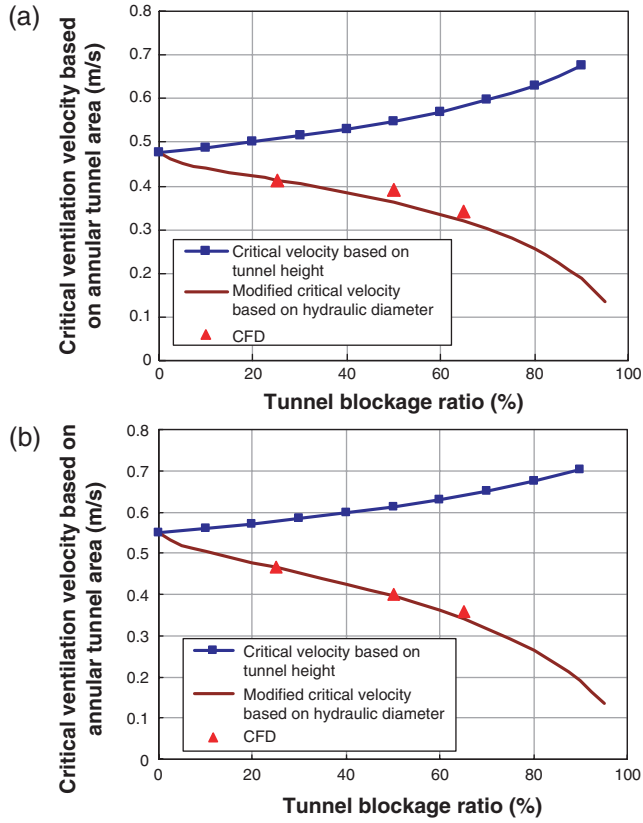

Figure 10. *Comparison of critical ventilation velocity as a function of blockage ratio, at HRR: (a) 7.5 kW and (b) 15 kW. (The color version of this figure is available on-line.)*

that is,

$$V_c \sim K_g^{3/2}\left(\frac{gH_D}{Fr_c}\right)^{1/2} \tag{21}$$

based on annular area hydraulic diameter, or

$$V_c \sim K_g^{3/2}\left(\frac{gH}{Fr_c}\right)^{1/2} \tag{22}$$

based on tunnel height.

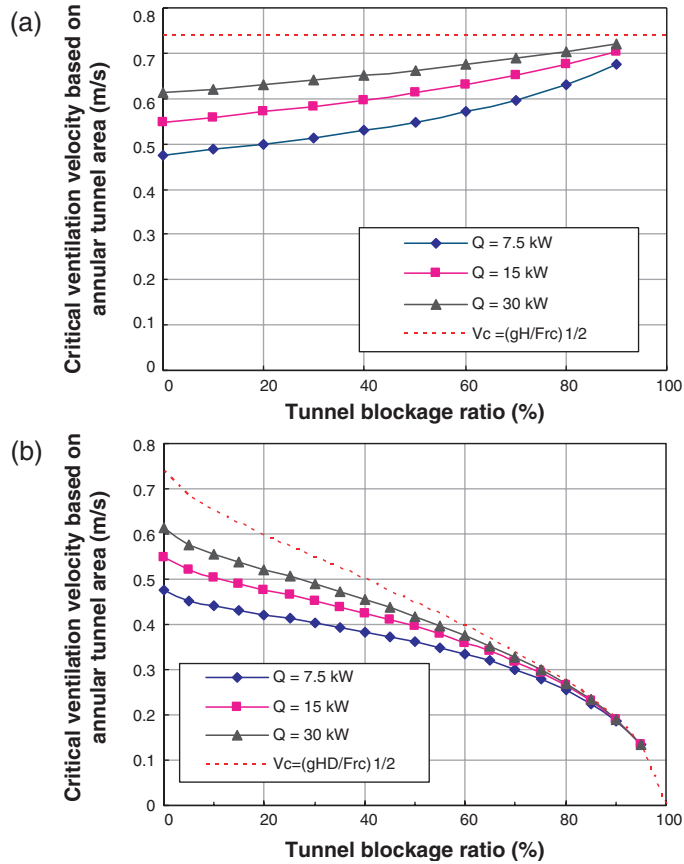

Figure 11. *The effect of HRR and blockage ratio on critical ventilation velocity: (a) based on tunnel height [1] and (b) based on hydraulic diameter. Dashed line is as* $Q \rightarrow \infty$. *(The color version of this figure is available on-line.)*

Both Equations (21) and (22) are consistent with Froude scaling [26], that is, $V \propto L^{1/2}$. The results from these two equations are shown as a dashed line in Figure 11. Because $T_f \gg T_0$ implies HRR goes to infinity, $Q \rightarrow \infty$, both equations give the limiting value of CV that depends on the characteristic length scale. However, the length scale associated with the enclosure obstruction is not represented in the correlation using tunnel height (Equation (22)), and it deviates from the limiting case of 100% blockage (Figure 11(a)). While HRR is an important factor in fire safety [27], the result from Equation (21) suggests that the geometrical factor could also be important. The higher HRR in tunnel fires, as opposed to the fires in an open environment, is another example [4].

Enclosure Fire in a Tunnel with Additional Blockage

The tunnel enclosure fire considered so far has only a single enclosure obstruction. In analogy to multiple-car trains, the effect of additional blockage is evaluated here, by adding a solid blockage either upstream or downstream of the enclosure (Figure 5(a)). For an HRR of 7.5 kW, and blockage ratio of 50%, the numerical result for CV is 0.195 m/s based on the entire tunnel cross-sectional area; whereas CV increases to 0.21 m/s for an additional upstream blockage, and 0.22 m/s for a downstream blockage.

For downstream blockage, the effect of ventilation velocity on the distribution of CO_2 mass fraction is shown in Figure 12. The plane is 10 mm below the tunnel ceiling, with the fire source projected as the circle. At lower velocities of 0.20 and 0.21 m/s, slight CO_2 backlayering can be seen. Critical velocity is taken as 0.22 m/s, because backlayering does not occur beyond the fire source. This suggests that a higher ventilation rate might be needed with additional blockage. However, the velocity of 0.22, or 0.44 m/s based on the annular area, is below the limiting 0.45 m/s from Equation (21), and

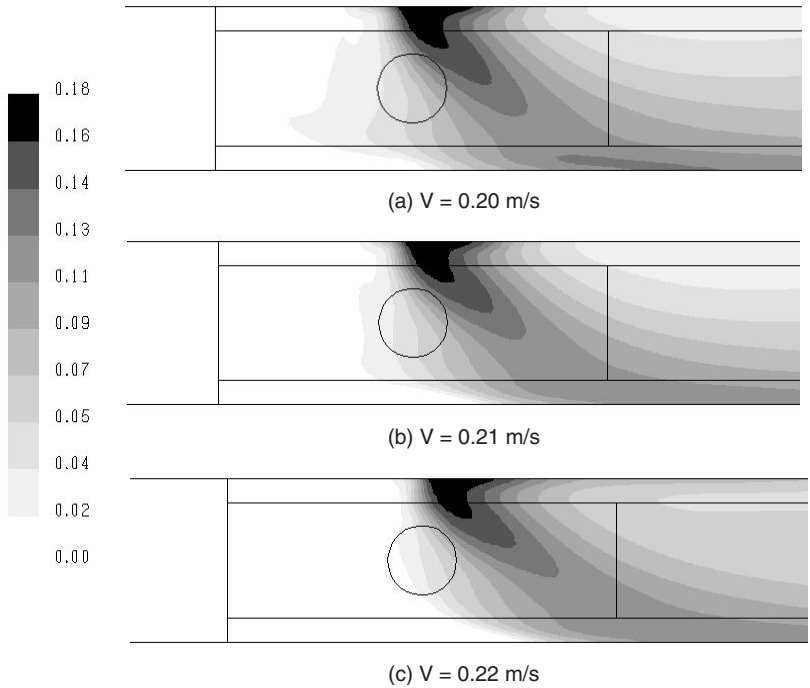

Figure 12. *Distribution of CO_2 mass fraction under three ventilation rates; an additional downstream blockage is included, and the plane is 10 mm below tunnel ceiling, $Q = 7.5$ kW.*

is well below 0.55 m/s based on tunnel height (Equation (7)). Note that as backlayering is caused by flow reversal, the change in CO_2 distribution is a direct result from the underlying flow field.

Effective Heat Release Rate in the Enclosure under Critical Velocity

The mixture fraction approach takes into account the oxygen availability, which is in contrast to VHMS with HRR as an input. The confined environment of an enclosure fire within a tunnel is likely to have incomplete combustion, that is, less than 100% in burning efficiency. From the numerical results, the ratio of the effective HRR in the enclosure to the total HRR is calculated under critical velocity conditions (Figure 13). This ratio is estimated from the *unburnt* fuel mass flow rate out of the door. The effective HRR ratio varies from 35 to 78% for the three blockage ratios examined. The highest ratio occurs at a blockage ratio of 50%. Slightly lower percentages can be seen with an additional blockage either upstream or downstream of the enclosure.

The geometrical effect on burning efficiency is demonstrated, as the effective HRR ratios for a 15 kW fire are significantly lower than those for 7.5 kW. The increase in effective HRR from blockage ratio 25 to 50% may come from the increase in the enclosure internal volume, and the

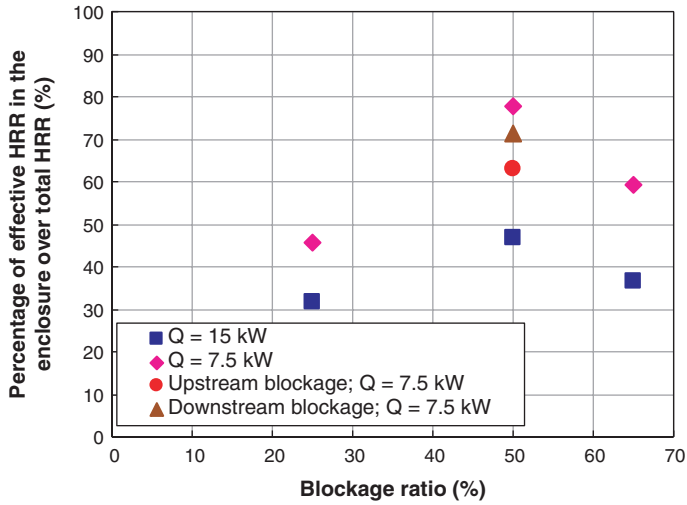

Figure 13. *Effective HRR in the enclosure under critical velocity conditions; percentage is estimated from unburnt fuel flowing out of the door. (The color version of this figure is available on-line.)*

decrease from 50 to 65% is probably because of the tighter restriction in the annular area. These percentages are qualitative, however, given the limitations of PDF in modeling fire physics (e.g., flammability), and given that test data on combustion efficiency is limited for an enclosure fire within a tunnel.

Discussion

As shown, the correlation based on hydraulic diameter predicts a significantly lower CV than that based on tunnel height, especially at higher blockage ratios. Oka and Atkinson [23] studied the effect of tunnel blockage in a small-scale experiment, which is based on the full-scale fire test at Health and Safety Laboratory (HSL), Buxton, UK. Using a raised propane gas burner supported by solid blockages, the experiment showed a 40–45% decrease in CV at 32% blockage, and an approximately 15% decrease at 12% blockage. The decrease in CV is significant, despite the fact that the fire is not an enclosure fire, but rather an external fire in an obstructed tunnel section. Nevertheless, the reported percentages of the decrease in CV [23] are consistent with those from the correlation based on hydraulic diameter (Equation (17)).

On the other hand, using an hydraulic diameter in a CV correlation is not new. This has been suggested, as in Equations (10) and (11) by Wu and Bakar [11], to account for the aspect ratio of the tunnel cross section. Previous studies have proposed other modifications, such as an additional parameter in Equation (8) [8]. The results on the near field effects [12] suggested $H^{3/2}/W^{1/2}$ as the representative length scale. As pointed out by Grant et al. [3], current practice in tunnel longitudinal ventilation may be conservative in some circumstances. This study suggests that the use of an hydraulic diameter may provide a quantitative correlation of CV and enclosure obstruction (Equation (17)). However, experimental validation will be needed to confirm the generality of the proposed correlation. Full-scale field tests will better represent the complex nature of this problem in practice, as the discussion here emphasizes a theoretical understanding based on data from small-scale experiments. Further investigation of enclosure fires in tunnels should include other factors, such as the aspect ratio of the tunnel cross section and the enclosure opening factor.

CONCLUSIONS

For longitudinal ventilation control of a tunnel fire, critical velocity is the minimum ventilation velocity to prevent smoke backlayering. In this article,

the effect of an enclosure obstruction is studied using a tunnel enclosure fire model. The results are summarized as follows:

- The numerical models are verified using experimental results from an enclosure fire and a tunnel fire. This ensures the numerical accuracy when the same approach is applied to an enclosure fire within a tunnel.
- To account for enclosure obstruction, the hydraulic diameter of the tunnel annular area is proposed as the characteristic length scale in the critical velocity correlation. The difference in the calculated critical velocity, compared to that based on tunnel height, increases significantly as enclosure blockage ratio increases. The results based on hydraulic diameter are consistent with the numerical results at blockage ratios of 25, 50, and 65%.
- The limiting case, as fire heat release rate goes to infinity, is evaluated for both the correlations based on either hydraulic diameter or tunnel height; while that based on hydraulic diameter seems reasonable as a function of blockage ratio.
- With additional solid blockage either upstream or downstream of the enclosure, the numerical results indicate that a higher critical velocity might be needed.
- The percentage of the effective heat release rate occurring inside the enclosure shows that the enclosure blockage ratio could have a significant effect on burning efficiency.
- Experimental validation will be needed to confirm the generality of using hydraulic diameter as the characteristic length scale.

NOMENCLATURE

C_p = specific heat (J/kg K)
g = gravitational force (m/s^2)
u = velocity (m/s)
k = turbulence kinetic energy (m^2/s^2)
R_{AF} = air–fuel mass ratio, dimensionless
f = mixture fraction, dimensionless
T_0 = ambient air temperature (K)
T = air temperature (K)
I = radiant intensity (W/m^2)
s = radiation path (m)
Q = fire heat release rate (W)
h_0 = elevation of neutral layer (m)
h = door height (m)

H = tunnel height (m)
Fr_c = critical Froude number, dimensionless
Fr_m = modified Froude number, dimensionless
T_f = gas temperature from fire (K)
ΔT = temperature difference from ambient (K)
K_g = tunnel grade correction factor, dimensionless
Q^* = dimensionless fire heat release rate
V_c^* = dimensionless critical ventilation velocity
H_D = tunnel hydraulic diameter (m)
W = tunnel width (m)
A = tunnel cross-sectional area (m^2)
A_b = tunnel blockage area (m^2)
A_a = tunnel annular area (m^2)
V_c = critical ventilation velocity (m/s)
V = ventilation velocity (m/s)

Greek

ρ_0 = ambient air density (kg/m^3)
ρ = air density (kg/m^3)
ε = turbulent dissipation (m^2/s^3)
μ_t = turbulent viscosity (kg/m s)
σ = Stefan–Boltzmann constant ($5.672 \times 10^{-8}\ W/m^2\,K^4$).
ϕ = tunnel blockage ratio, dimensionless
ω = tunnel grade (%)

REFERENCES

1. US DOT Federal Transit Administration, Subway Environmental Design Handbook, Vol. II, Subway Environment Simulation (SES) Computer Program, Version 4, Part I, User's Manual, FTA-MA-26-7022-91-1, 1997.
2. Kennedy, W.D., Gonzalez, J.A. and Sanchez, J.G., "Derivation and Application of the SES Critical Velocity Equations," In: ASHRAE Summer Annual Meeting, San Antonio, TX, USA, 1996.
3. Grant, G.B., Jagger, S.F. and Lea, C.J., "Fire in Tunnels," Phil. Trans. R. Soc. Lond. A., Vol. 356, 1998, pp. 2873–2906.
4. Carvel, R.O., Beard, A.N., Jowitt, P.W. and Drysdale, D.D., "The Influence of Tunnel Geometry and Ventilation on the Heat Release Rate of a Fire," Fire Tech., Vol. 40, No. 1, 2004, pp. 5–26.
5. Massachusetts Highway Department/Federal Highway Administration, Memorial Tunnel Fire Ventilation Test Program, Phase IV Report, 1999.
6. Rhodes, N., "Smoke Modelling," In: 1 Day Seminar on Smoke and Critical Velocity in Tunnels, Organized by Independent and Technical Conferences, London, UK, 1996.

7. Kennedy, W.D. and Kang, K., "Tunnel Fire Modeling Comparing CFD and the Froude Number Method," In: Proceedings of the 11th BHR Group International Symposium on Aerodynamics and Ventilation of Vehicle Tunnels, Luzern, Switzerland, 2003.
8. Tetzner, D., Pollak, R., Foit, W. and Sippel, M., "Critical Velocity – Comparative Assessment of Test Results and CFD Simulation," In: Proceedings of the International Conference on Tunnel Fire and Escape from Tunnels, Lyon, France, 5–7 May 1999, pp. 181–190.
9. Kunsch, J.P., "Simple Model for Control of Fire Gases in a Ventilated Tunnel," Fire Safety J., Vol. 37, No. 1, 2002, pp. 67–81.
10. Kunsch, J.P., "Critical Velocity and Range of a Fire-Gas Plume in a Ventilated Tunnel," Atmospheric Environment, Vol. 33, No. 1, 1999, pp. 13–24.
11. Wu, Y. and Bakar, M.Z.A., "Control of Smoke Flow in Tunnel Fires Using Longitudinal Ventilation Systems – A Study of the Critical Velocity," Fire Safety J., Vol. 35, No. 4, 2000, pp. 363–390.
12. Kurioka, H., Oka, Y., Satoh, H. and Sugawa, O., "Fire Properties in Near Field of Square Fire Source with Longitudinal Ventilation in Tunnels," Fire Safety J., Vol. 38, No. 4, 2003, pp. 319–340.
13. Steckler, K.D., Quintiere, J.G. and Rinkinen, W.J., "Flow Induced by Fire in a Compartment," National Bureau of Standards, NBSIR 82-2520, 1982.
14. Xue, H., Ho, J.C. and Cheng, Y.M., "Comparison of Different Combustion Models in Enclosure Fire Simulation," Fire Safety J., Vol. 36, No. 1, 2001, pp. 37–54.
15. Lewis, M.J., Moss, M.B. and Rubini, P.A., "CFD Modeling of Combustion and Heat Transfer in Compartment Fires," In: Proceedings of the 5th International Symposium on Fire Safety Science, IAFSS, 1997, pp. 463–474.
16. McGrattan, K.B., Baum, H.R. and Rehm, R.G., "Large Eddy Simulation of Smoke Movement," Fire Safety J., Vol. 30, No. 2, 1998, pp. 161–178.
17. Fluent Inc., Fluent v6.1 User's Guide, Lebanon, NH, 2003.
18. Zigh, A., Ong, I. and Kang, K., "CFD Applications for Subway Stations," In: Proceedings of the 10th BHR Group International Symposium on Aerodynamics and Ventilation of Vehicle Tunnels, Boston, Massachusetts, USA, 2000.
19. Jones, W.P. and Whitelaw, J.H., "Calculation Methods for Reacting Turbulent Flows: A Review," Combust. Flame, Vol. 48, 1982, pp. 1–26.
20. Floyd, J.E., McGrattan, K.B., Hostikka, S. and Baum, H.R., "CFD Fire Simulation Using Mixture Fraction Combustion and Finite Volume Radiative Heat Transfer," J. of Fire Protection Engineering, Vol. 13, No. 1, 2003, pp. 11–36.
21. Coppalle, A. and Vervisch, P., "The Total Emissivities of High-Temperature Flames," Combust. Flame, Vol. 49, 1984, pp. 101–108.
22. Thermal Ceramics, Data Sheet, http://www.thermalceramics.com/home.html.
23. Oka, Y. and Atkinson, G.T., "Control of Smoke Flow in Tunnel Fires," Fire Safety J., Vol. 25, No. 4, 1995, pp. 305–322.
24. Megret, O., Vauquelin, O. and Casale, E., "An Experimental Study of Critical Velocity and the Influence of Source Diameter," In: Proceedings of the International Conference on Tunnel Fire and Escape from Tunnels, Lyon, France, 5–7 May 1999, pp. 429–435.
25. Thomas, P.H., "The Movement of Smoke in Horizontal Passages against an Airflow," Fire Research Station Note No. 723, Fire Research Station, UK, 1968.
26. NFPA-92B, Guide for Smoke Management Systems in Malls, Atria, and Large Areas, 2000 Edition, National Fire Protection Association, Quincy, MA.
27. Babrauskas, V. and Peacock, R.D., "Heat Release Rate: The Single Most Important Variable in Fire Hazard," Fire Safety J., Vol. 18, No. 3, 1992, pp. 255–272.